ARMY RESEARCH LABORATORY

ARL

Modified Hyperbranched Polymers for Fluorescence Sensing Applications

by Joshua A. Orlicki, Xianyan Wang, Matthew S. Bratcher,
Robert E. Jensen, Lynne A. Samuelson, and Steven H. McKnight

ARL-TR-6018   **June 2012**

NOTICES

Disclaimers

The findings in this report are not to be construed as an official Department of the Army position unless so designated by other authorized documents.

Citation of manufacturer's or trade names does not constitute an official endorsement or approval of the use thereof.

Destroy this report when it is no longer needed. Do not return it to the originator.

Army Research Laboratory

Aberdeen Proving Ground, MD 21005

Modified Hyperbranched Polymers for Fluorescence Sensing Applications

Joshua A. Orlicki, Matthew S. Bratcher, Robert E. Jensen,
and Steven H. McKnight
Weapons and Materials Research Directorate

Xianyan Wang
University of Massachusetts Lowell

Lynne A. Samuelson
U.S. Army Natick Soldier Research, Development, and Engineering Center

REPORT DOCUMENTATION PAGE

1. REPORT DATE (DD-MM-YYYY)	2. REPORT TYPE	3. DATES COVERED (From – To)
June 2012	Final	March 2003–August 2004

4. TITLE AND SUBTITLE	5a. CONTRACT NUMBER
Modified Hyperbranched Polymers for Fluorescence Sensing Applications	
	5b. GRANT NUMBER
	5c. PROGRAM ELEMENT NUMBER

6. AUTHOR(S)	5d. PROJECT NUMBER
Joshua A. Orlicki, Xianyan Wang,[*] Matthew S. Bratcher, Robert E. Jensen, Lynne A. Samuelson,[†] and Steven H. McKnight	
	5e. TASK NUMBER
	5f. WORK UNIT NUMBER

7. PERFORMING ORGANIZATION NAME(S) AND ADDRESS(ES)	8. PERFORMING ORGANIZATION REPORT NUMBER
U.S. Army Research Laboratory ATTN: RDRL-WMM-G Aberdeen Proving MD 21005	ARL-TR-6018

9. SPONSORING/MONITORING AGENCY NAME(S) AND ADDRESS(ES)	10. SPONSOR/MONITOR'S ACRONYM(S)
	11. SPONSOR/MONITOR'S REPORT NUMBER(S)

12. DISTRIBUTION/AVAILABILITY STATEMENT

Approved for public release; distribution unlimited.

13. SUPPLEMENTARY NOTES

[*]Center for Advanced Materials, University of Massachusetts Lowell, Lowell, MA 01854
[†]U.S. Army Natick Soldier Research, Development, and Engineering Center, Natick, MA 01760

14. ABSTRACT

During this research, this study employed commercially available hyperbranched polymers (HBPs) modified with aliphatic, perfluorinated, and fluorescent moieties to yield polyesters with controlled end group functionality. Similar polymers have migrated to the surface of cast polymer films when incorporated as a minor constituent of a linear polymer film. The polymers were incorporated into polyacrylonitrile and poly(2-hydroxyethyl methacrylate) matrices and were shown to function as fluorescence sensors. The HBPs transported the fluorescent groups to the fiber mat surface where they interacted with mercury (Hg(II)) or cytochrome c as the analyte. Sensitivities were modest and showed linear response with Hg(II) as the quenching agent and nonlinear response with cytochrome c. This work suggests that HBPs may provide a broadly accessible scaffold for the introduction of fluorescence-sensing elements in nonreactive polymer matrices.

15. SUBJECT TERMS

hyperbranched polymer, fluorescence sensing, quenching, heavy metal

16. SECURITY CLASSIFICATION OF:			17. LIMITATION OF ABSTRACT	18. NUMBER OF PAGES	19a. NAME OF RESPONSIBLE PERSON
a. REPORT	b. ABSTRACT	c. THIS PAGE			Joshua A. Orlicki
Unclassified	Unclassified	Unclassified	SAR	26	19b. TELEPHONE NUMBER (Include area code) (410) 306-0931

Contents

List of Figures

List of Tables

Preface

The work detailed here was conducted several years ago, and some of the authors have changed affiliations since. Steven H. McKnight, then a branch chief at the U.S. Army Research Laboratory's Weapons and Materials Research Directorate, is now with the National Science Foundation. Xianyan Wang, then with the University of Massachusetts, is now with Organogenesis, Inc.

Acknowledgments

1. Introduction

The development of highly sensitive detection techniques for chemical and biochemical agents continues to be a major challenge because of the increasing demands for faster, simpler, and less expensive detection methods. In recent years, a number of ultrasensitive fluorescent optical sensors for a variety of analytes have been demonstrated (*1–3*).

We have previously reported on the use of electrospun polymer membranes containing a fluorophore to yield a highly responsive fluorescent optical sensors (*4, 5*). These sensors had Stern-Volmer constant (K_{sv}) values in excess of 10^5, which were 2 to 3 orders of magnitude higher than those from thin films made from the same sensing material. We attribute this increase in sensitivity to the inherently high surface-area-to-volume ratio found in electrospun membranes. Electrospinning is a relatively simple and versatile method for creating high surface area fibrous polymer membranes. In a typical process, a large static voltage is applied to a polymer solution to generate fine jets of solution that dry into an interconnected membrane-like web of small fibers (*6*). The fiber diameters are generally in the range of 10–1000 nm. Electrospun nanofibrous membranes can have surface areas ~1 to 2 orders of magnitude higher than those of continuous thin films. It is expected that applications such as sensors and catalysts, where large surface areas are desired, can benefit from the use of electrospun membranes to improve performance.

The sensitivity of fluorescence quenching-based optical sensors can be dramatically affected by the accessibility of the sensing elements to the quencher, or analyte. Although electrospun fluorescent membranes have shown significantly improved sensitivities over continuous thin films (*4*), there remains room for improvement. Typically, the mean diameter of the electrospun fibers in our experiments was between 100 to 400 nm, thus limiting diffusion of the quencher to fluorophores located in the interior of the fiber (*1*). To address this limitation, scientists have employed a number of novel approaches to localize and immobilize the fluorescent sensing elements onto the surface of the electrospun fibers (*7, 8*). The sensors made by these methods had both the high surface-area-to-volume ratio of the electrospun membranes and optimal exposure of the fluorescent sensing element to the quenchers. This in turn led to higher device sensitivities.

An alternative approach to the modification of the electrospun fiber surfaces is to develop sensing additives that spontaneously establish a concentration gradient in the fiber. By thermodynamically driving the segregation of the sensing moiety to the surface, we may increase the sensitivity of the fiber and employ lower total levels of fluorophores. The use of low surface energy sensor materials permits the preferential surface segregation of the sensor, increasing its concentration at the film surface. Several groups have showed selective surface segregation for linear polymer systems, especially for polystyrene substrates with oligomeric fluorinated chains.

Fluorinated combs were shown to segregate to the surface (*9*), as were block copolymers with fluorinated chain ends (*10, 11*). Triblock polymers have also shown the ability to control substrate properties and provide a means for a responsive surface (*12*).

Dendritic and hyperbranched polymers (HBPs) represent materials with high functionality and straightforward routes of modification. It is well known that changing the end groups of an HBP shifts its physical properties, such as solubility or glass transition temperature (T_g) (*13, 14*). Surface properties are also modified (*15–18*) by the identity of end groups. Both the oxygen permeability (*19*) and the water uptake (*17*) of HBP polyester films were found to depend on end-group characteristics.

When HBPs with low energy end groups were blended with linear polymers, they were also observed to segregate preferentially at the film surface. Schmaljohann et al. (*20*) have used the amphiphilic interior of alkyl-terminated polyesters to sequester dye molecules to color polyolefins. Hong and coworkers (*21, 22*) used similar polyesters to prepare extruded rods and blown films, and observed changes in the gloss and surface properties of the extruded surface. Also, the use of modified HBPs to control the surface properties of cast films has been reported (*23–26*).

Fluorescent molecules have also been attached to dendritic polymers. Typically, they are incorporated as the focal point of a dendritic antenna, funneling photons to the fluorophore and enhancing its fluorescence. Pugh and coworkers (*27, 28*) have employed fluorescence quenching using a binol-based dendrimer sensor, which exhibited differential sensitivity to enantiomeric amino alcohols.

We have incorporated many of these principles and have developed a hyperbranched polymer that spontaneously segregates to a film surface to deliver a fluorescent group for sensing applications. We have also evaluated hyperbranched polymers with pyrenebutyric acid (PBA) end groups as sensors to detect cation-induced quenching. This approach uses the hyperbranched polymer scaffold to deliver a sensing group to a substrate surface and is presented here as a unique application for highly branched macromolecules. We expect that this localization of the fluorescent tag to the surface of a high surface area nanofibrous membrane would further improve sensitivity and reversibility compared to similar systems in which the fluorescent polymer was dispersed throughout the electrospun nanofibers. This approach also allows for more direct control over the concentration of fluorophore that was ultimately used.

2. Experimental Procedures

2.1 Materials

Hyperbranched polyesters were obtained from Perstorp Corp. Perfluorooctanoic acid was obtained from Exfluor Research Group. Other materials were obtained from Alfa-Aesar or VWR and were used as received without further purification.

2.2 Characterization Techniques

Nuclear magnetic resonance spectroscopy was carried out using a Bruker-Biospin 600-MHz Ultrashield Avance spectrometer, equipped with a broadband probe and 5-mm outer diameter tubes (32 scans, 15-s d1). Spectra were obtained in deuterated chloroform ($CDCl_3$) at room temperature, and all resonances are reported as parts per million (ppm) referenced to the residual solvent peak (δ 7.26 ppm for $CDCl_3$). Carbon spectra were obtained using the attached proton test pulse sequence, allowing the unambiguous assignment of carbon multiplicity. Polymer molecular weight was determined by gel permeation chromatography (GPC) using a linear mixed bed column along with 50- and 500-Å cross-linked styrene columns employing refractive index (RI) and multiangle laser light-scattering (MALLS) detection. The RI detector was a Wyatt Technologies Optilab, while the MALLS detector was a Wyatt DAWN EOS 18-angle detector. Samples were analyzed using the ASTRA software package. Differential refractive index (RI) values (dn/dc) for the HBPs were determined for polymer 3, employing the Wyatt dn/dc Windows software package and solutions of known concentration analyzed with the RI detector fed via syringe pump. The value for dn/dc of polymer 3 was 0.084 ± 0.003. Molecular weights were determined assuming constant dn/dc values for polymers 1–3.

Contact angles were recorded using a goniometer equipped with a charge-coupled device camera and an image capture program set up via LabVIEW software. Contact angles were measured using Millipore water by defining a circle about the drop and recording the tangent angle formed at the substrate surface.

X-ray photoelectron spectroscopy (XPS) was carried out with VG ESCALAB (VG Scientific Lit.) using $MgK\alpha$ radiation (hν = 1253.6 eV) as the excitation source. The morphology of the membranes was determined using an Amray 1400 scanning electron microscope (accelerating voltage 10 kV). The sensing capabilities of the membranes were determined by measuring the fluorescence quenching in the presence of the analyte with a Perkin Elmer LS 55 fluorescence spectrofluorometer. The electrospun membrane-coated glass slides were fixed in a 1-cm quartz cuvette that was filled with the analyte solution. The excitation wavelength used was 340 nm, and the emission spectra were measured from 370 to 580 nm.

2.3   Electrospinning

Electrospinning was used to fabricate optical chemical sensors. Electrospinning is accomplished by forcing a spin-dope solution of polymer through a syringe that has a voltage applied to it. Electrostatic repulsion causes the solution to separate into several streams upon exiting the syringe. The solvent is driven off rapidly due to the small diameter/high surface area of the resulting fibers, which are collected as an unoriented mat on a grounded plate.

The spin-dope solution consisted of HPB-PBA and poly(2-hydroxyethyl methacrylate) (PHEMA) dissolved in a 2:1 ratio of methanol/dimethylformamide (DMF), or polyacrylonitrile(PAN) dissolved in DMF. For each HPB-PBA, four different films were prepared for quenching studies in order to investigate the effect of concentration of HPB-PBA and polymer matrix on the sensitivity of sensor. Each film was prepared under almost the same conditions.

A live electrode wire from the DC power source (Gamma High Voltage Research, Inc., model HV ES30P/100) was inserted into the pipette, which contained the spin dope (figure 1). The interior diameter of the glass pipette capillary tip ranged from 1.2 to 1.5 mm. The charged polymer solution overcame the surface tension of the liquid, and a multitude of polymer jets was produced. The solvent evaporated, and very fine fibers were collected on a glass slide. The applied electrospinning voltages ranged from 15 to 20 kV. The working distance between the tip of the pipette and the glass slide was typically 15 to 20 cm. The collection time was about 30 to 45 s. The electrospun membranes were dried in an oven at 70 °C for 24 h.
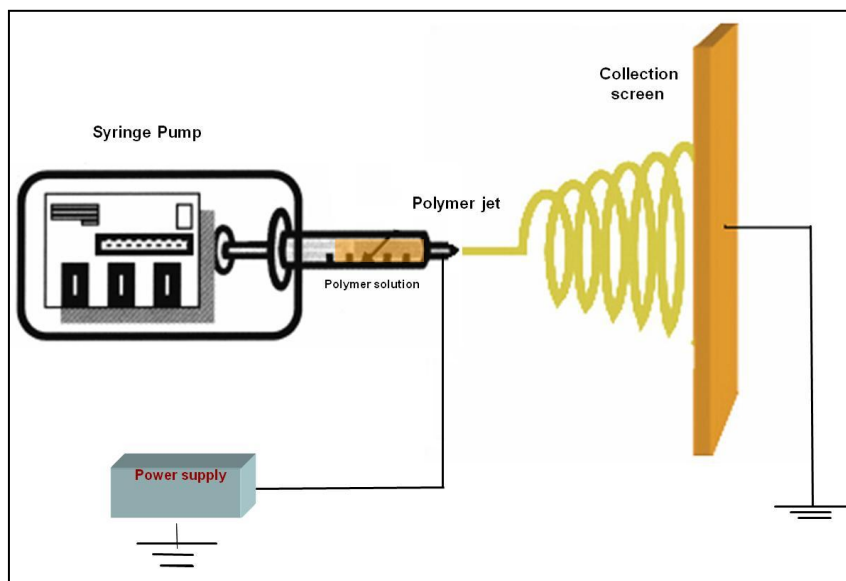

Figure 1. Schematic of electrospinning assembly.

2.4   Representative Procedure: HBP Modification

A hyperbranched polyester (1.0 g, 8.61 mmol hydroxy groups) and dodecanoic acid (0.52 g, 0.3 equiv, 2.6 mmol) were charged to a 40-mL vial equipped with a magnetic stir bar. The vial was placed into an oil bath at 140 °C and purged with a nitrogen stream. After ~10 min, the contents of the vial had melted to form a homogenized solution. One drop (~0.1 mL) of concentrated sulfuric acid was added, and the reaction timer was begun. After 1 h, the vial was uncapped and the remaining solid reagents were added, including perfluorooctanoic acid (1.42 g, 0.4 equivalent, 3.4 mmol) and PBA (0.49 g, 0.2 equivalent, 1.7 mmol). The vial was capped and maintained under a constant N_2 stream, and was stirred vigorously for 3.5 h. Then the vial was removed from heat and the stir bar was removed from the molten polymer. Upon cooling, the polymer formed a dark, viscous oil. The recovered mass was 2.52 g (76%). Characterization data for the polymers is as follows:

Polymer 1: ^{1}H NMR (600 MHz, CDCl$_3$, δ): 8.28-7.82 (pyrene CH, 6.1 H), 4.51 (-OH, 1.6 H), 4.24 (CH$_2$-ester, 9 H), 3.62-3.33 (CH$_2$-OH, 10.3 H), 2.44 (CH$_2$, 1.4 H), 2.28 (CH$_2$, 2.1 H), 2.11 (CH$_2$, 1.5 H), 1.57 (CH$_2$, 2.1 H), 1.26 (CH$_2$, 25.6 H), 0.87 (CH$_3$, 3 H); ^{13}C NMR (150 MHz, CDCl$_3$, δ): 173.5-172.7 (carbonyl), 135.4 (CH$_2$), 131.3 (CH$_2$), 130.8 (CH$_2$), 129.9 (CH$_2$), 128.6 (CH$_2$), 127.5 (aromatic CH), 126.7 (aromatic CH), 125.8 (aromatic CH), 124.7 (aromatic CH), 123.1 (aromatic CH), 34.0-33.5 (CH$_2$), 29.6-29.3 (CH$_2$), 26.6 (CH$_2$), 24.9 (CH$_2$), 22.6 (CH$_2$), 17.6 (-CH$_3$). M_n = 18.5 kDa, Mw = 22.8 kDa. NOTE: using assumed dndc of 0.084.

Polymer 2: ^{1}H NMR (600 MHz, CDCl$_3$, δ): 8.30-7.85 (pyrene CH, 0.6 H), 4.50 (-OH, 2.8 H), 4.24 (CH$_2$-ester, 6.1 H), 3.63-3.44 (CH$_2$-OH, 5.1 H), 2.30 (CH$_2$, 2.2 H), 1.56 (CH$_2$, 2.0 H), 1.24 (CH$_2$, 22.3 H), 0.87 (CH$_3$, 3.0 H); ^{13}C NMR (150 MHz, CDCl$_3$, δ): 173.9-171.2 (carbonyl), 159.2, 157.4, 131.4 (CH$_2$), 131.0 (CH$_2$), 129.9 (CH$_2$), 128.7 (CH$_2$), 127.4 (aromatic CH), 126.8 (aromatic CH), 125.8 (aromatic CH), 124.7 (aromatic CH), 112.2, 110.3, 108.2, 106.3, 48.6 (CH$_2$), 46.6 (CH$_2$), 34.0 (CH$_2$), 31.9 (CH$_2$), 29.6-29.1 (CH$_2$), 24.8 (CH$_2$), 22.7 (CH$_2$), 17.6 (-CH$_3$), 14.1 (–CH3). M_n = 20.4 kDa, Mw = 23.3 kDa. NOTE: using assumed dndc of 0.084.

Polymer 3: ^{1}H NMR (600 MHz, CDCl$_3$, δ): 8.29-7.85 (pyrene CH, 1.0 H), 4.24-4.19 (CH$_2$-ester, 3.7 H), 3.63-3.44 (CH$_2$-OH, 1.8 H), 2.29 (CH$_2$, 2.4 H), 1.58 (CH$_2$, 2.0 H), 1.24 (CH$_2$, 18.6 H), 0.87 (CH$_3$, 3.0 H); ^{13}C NMR (150 MHz, CDCl$_3$, δ): 173.2-171.4 (carbonyl), 131.4 (CH$_2$), 130.8 (CH$_2$), 130.0 (CH$_2$), 128.6 (CH$_2$), 127.4 (aromatic CH), 126.6 (aromatic CH), 125.8 (aromatic CH), 124.7 (aromatic CH), 123.2 (aromatic CH), 46.6 (CH$_2$), 46.3 (CH$_2$), 34.0 (CH$_2$), 31.9 (CH$_2$), 29.6-29.1 (CH$_2$), 24.8 (CH$_2$), 22.7 (CH$_2$), 17.7 (-CH$_3$), 14.1 (–CH3). M_n = 5.9 kDa, Mw = 8.2 kDa. NOTE: using assumed dndc of 0.084.

3. Results and Discussion

3.1 Synthesis

The modification of the HBP followed procedures previously reported in the literature (*29*). Monofunctional aliphatic acids were used to terminate the polymerization of bismethoxypropyl acid (bis-MPA). Hong and coworkers (*21, 22*) have investigated similar HBPs as additives to polyolefins for the modification of the surface of extruded films. The melt-phase condensation of specific acids to give modified chain ends was used to add both perfluorinated and fluorescent acids to the periphery of the HBP. Poor miscibility between the backbone and acids resulted in phase segregation even at elevated temperatures.

The degree of phase segregation was reduced or eliminated by the use of dodecanoic acid as an end group that also plasticized the polymer melt. A relatively low percentage of the aliphatic acid improved the miscibility of the HBP in total and permitted the attachment of perfluorinated or aromatic end groups onto the HBP. Figure 2 shows a typical procedure used to modify the end groups of the hyperbranched polyester. The polyester is modified by condensation with the desired acids at elevated temperatures under N_2 flow to remove evolved water. Note that the polyester is drawn to highlight the n+1 dependence of end group concentration and is not meant to imply a linear structure with pendant chains.
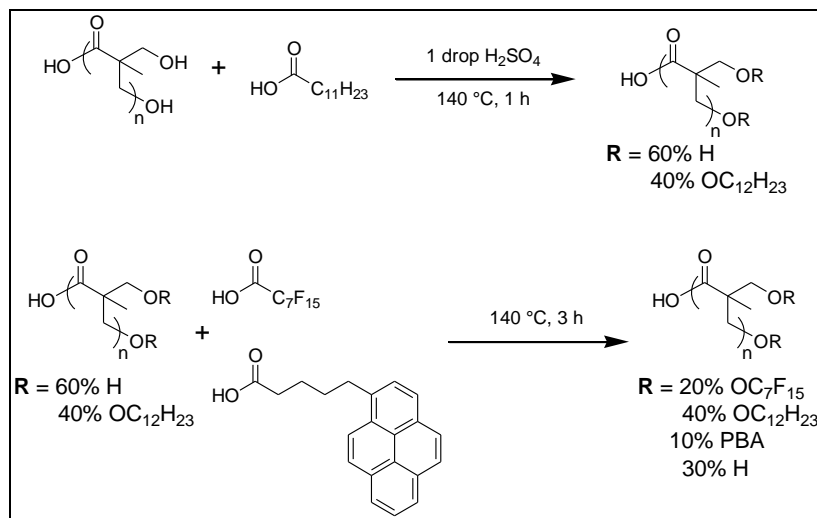
Figure 2. Preparation of modified polyesters.

The HBP was melted while under a stream of nitrogen gas, then the appropriate aliphatic acid plasticizer was added and the condensation was permitted to proceed for ~0.5–1 h. Additional acids were then added, and the homogenized mixture underwent condensation for the succeeding 3 h. The melt was maintained under a stream of nitrogen gas to remove water as it formed during the condensation reaction. The polymer was then removed from heat and allowed to cool.

Translucent or clear oils of varying viscosity were obtained from the end group modificiation. The polymer was used for studies without further purification.

The polymers were analyzed by nuclear magnetic resonance (NMR) spectroscopy as well as GPC molecular weight determination. The ^{1}H NMR analysis indicates the successful incorporation of aliphatic chains onto the HBP end groups. The approximate quantity of aromatic protons can also be determined, confirming the attachment of the PBA to the HBP. Carbon spectra were obtained to illustrate and catalog the various bonding states in the HBP backbone (e.g., several carbonyl resonances, several –CH_2- resonances from multiple backbone connectivities and end group arrangements). The molecular weights of the polymers were determined using gel permeation chromatography with MALLS detection. The MALLS laser emits light at 633 nm, outside the absorption range for the PBA fluorophore. The polymer chromatograms were also monitored at both 280 and 340 nm. The first wavelength would detect the carbonyl groups of the HBP backbone, while the longer wavelength would only be absorbed by PBA, allowing for the detection of any unbound PBA in the system. The chromatographs obtained at variable wavelengths indicated that very little unbound PBA remained in the system. Also, assuming a constant dn/dc value of the polymers of 0.084 (determined experimentally for polymer 3 {I-173c}) gave a range of molecular weights ranging from 5900 to 18,500 Da.

3.2   Electrospinning

Two polymer matrices were selected to prepare the electrospun membrane polymer blends. Both PHEMA and PAN were used as matrix materials. The base polymers were dissolved in 2:1 methanol/dimethylformamide MeOH/DMF or DMF (PHEMA and PAN, respectively), and sufficient HBP was added to provide loading levels of 1 and 4 weight-percent. Each spin dope solution was prepared as indicated in the experimental section. Compositions of the membranes are given in table 1, along with the resultant relative mass of the sensing moiety, the PBA.

The fluorescence characteristics of the blends were evaluated using samples 1-A, 2-A, and 3-A (figure 3). The membranes were exposed to incident light at 340 nm, and the resulting fluorescence arose from the PBA attached to the HBP additive. The fluorescence of 1-A shows the classic red shift of pyrene excimer formation, along with the loss of fine structure in the emission spectrum. Excimer formation is a consequence of pi-stacking of the pyrene rings in the excited state and is dependent upon concentration of the fluorophore. Excimer emission is the dominant source of fluorescence for 1-A. As the concentration of the PBA decreases in 2-A and 3-A, the excimer emission band is reduced in intensity and the characteristic emissions for pyrene are observed (376 and 397 nm).

Table 1. Composition of electrospun membrane materials.

Sample	HBP	Matrix	Mass% HBP	Mass% PBA
1-A	1	PHEMA	1	0.144
1-B	1	PHEMA	4	0.576
1-C	1	PAN	1	0.144
1-D	1	PAN	4	0.576
2-A	2	PHEMA	1	0.0772
2-B	2	PHEMA	4	0.309
2-C	2	PAN	1	0.0772
2-D	2	PAN	4	0.309
3-A	3	PHEMA	1	0.0199
3-B	3	PHEMA	4	0.0796
3-C	3	PAN	1	0.0199
3-D	3	PAN	4	0.0796

Note: "Mass % HBP" and "Mass % PBA" indicate percentage of total mass
that the HBP and covalently bound PBA contribute, respectively,
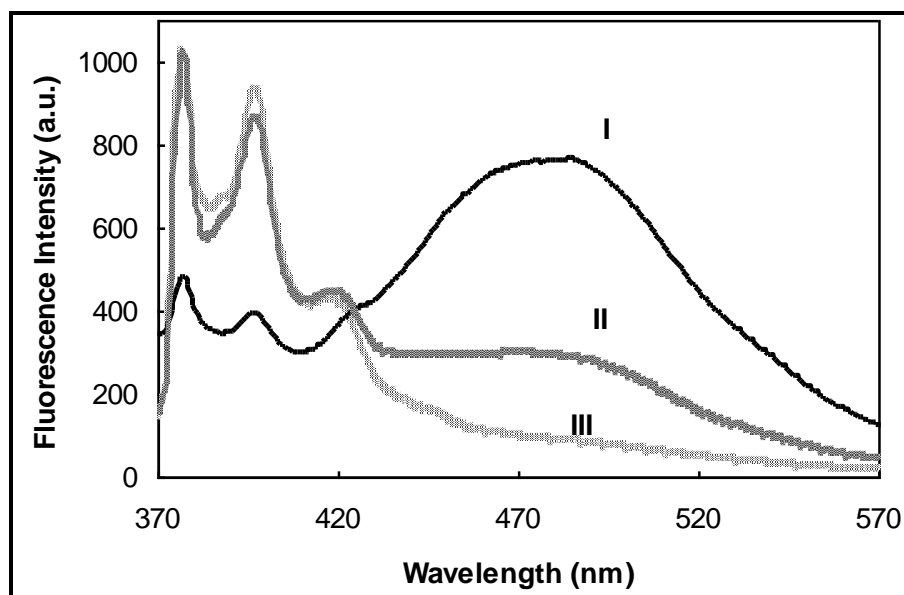relative to the matrix material.

Figure 3. Fluorescence characteristics of HBP-PBAs in linear polymer matrix.

The morphology of the membranes was evaluated using scanning electron microscopy micrographs (figure 4). The electrospun fibers were randomly oriented as a porous membrane, with a distribution of fiber diameters ranging between 100 and 500 nm. This type of porous structure provides a surface-area-to-volume increase of roughly 1 to 2 orders of magnitude relative to continuous thin films. Further increases of the surface-area-to-volume ratio may be achieved by changing the conditions of the electrospinning process. Conditions such as voltage, solvent, concentration, and working distance may be controlled to result in smaller diameter fibers, fewer beads, or increased porosity at the fiber surface. The control of film morphology is important for the optimization of sensing capabilities.
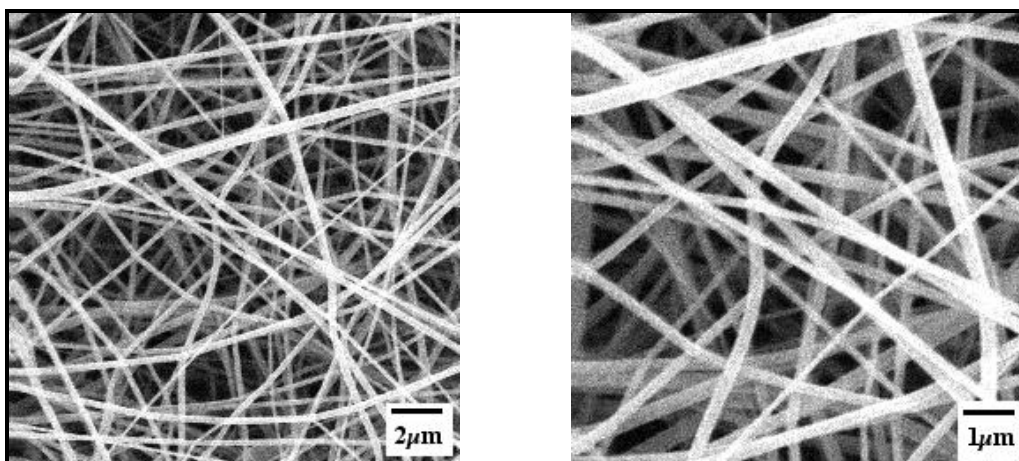

Figure 4. Electrospun fiber morphology.

The PBA-tagged HBPs were designed to preferentially segregate to the polymer/air interface. In addition to the fluorophore end groups, the HBP also contained end groups condensed from perfluorooctanoic acid, which provided the thermodynamic driving force for surface segregation. Fluorinated segments in polymer matrices may segregate to the polymer surface, minimizing the surface free energy of the film at the polymer/air interface (*30*). The use of perfluorinated segments to modify a surface is well known, especially when used to terminate block copolymers (*31*).

The surface properties of the electrospun membranes were also probed using angle resolved x-ray photoelectron spectroscopy. The surface segregation of the HBP was investigated by comparing the atomic compositions (carbon/fluorine ratio) at different takeoff angles (TOAs), which relate to the depth of penetration of the analysis. The sampling depth was directly proportional to sin(TOA), so a 90° TOA results in the deepest sampling depth (~10 nm). More acute TOAs (measured from the sample surface) reduce the depth from which the XPS information is obtained. By comparing the results, it is possible to infer the migration of the HBPs to the surface of the fibers.

The XPS measurements in figure 5 show the photoionization peaks of carbon, oxygen, and fluorine in a survey scan and in detail scans. The survey scan (A) shows the prevalence of C, O, and F as expected. Spectra B–D show expanded regions for C, F, and O, respectively. Note in B the peaks for CF2 and CF3 near 293 and 297 eV, respectively, and their intensity inversion as a function of TOA.
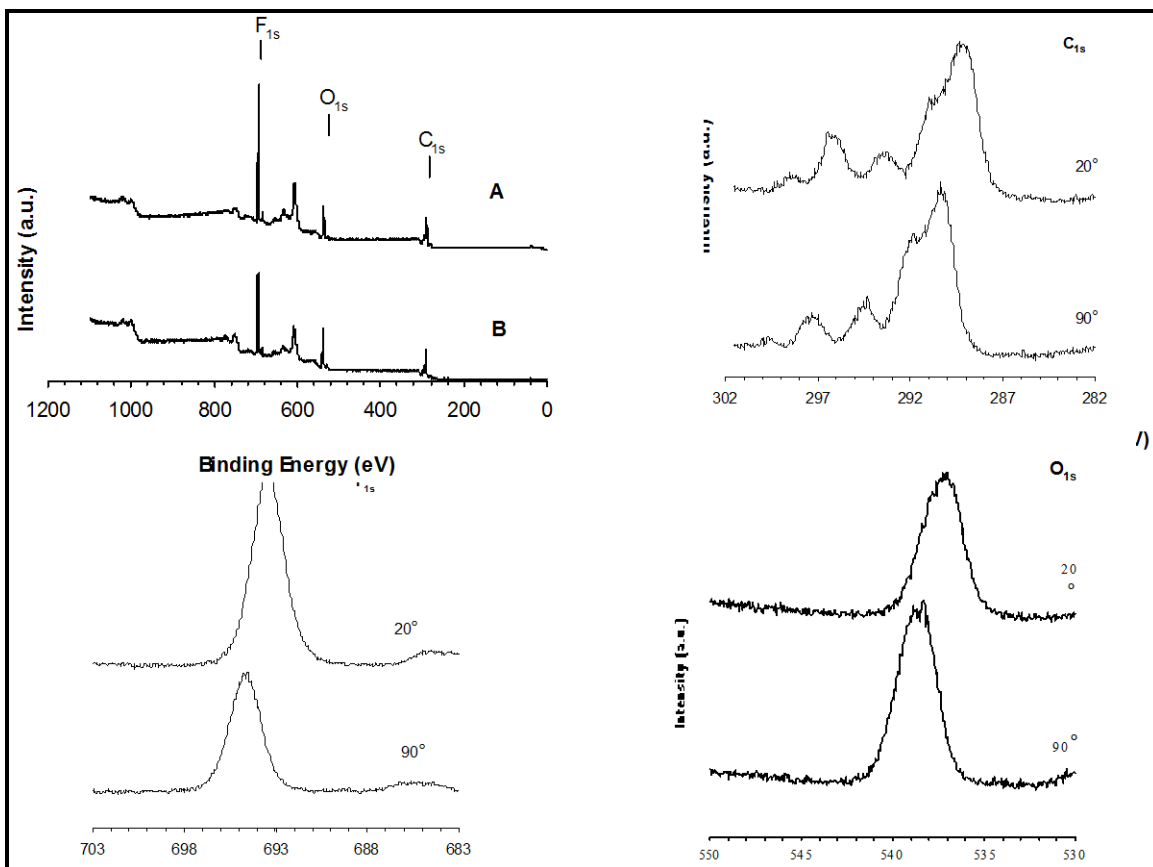

Figure 5. Surface composition of electrospun membranes.

Integrating the peak area provides values proportional to the number of atoms that contribute to the signal, so it is possible to determine the composition of a surface after accounting for the sensitivity of the nuclei of interest. The C:F ratio was found to vary with TOA. At a 90° TOA (perpendicular to film) the ratio was 1:0.45; at 20° TOA the ratio was 1:0.75. The increasing abundance of fluorine indicates enrichment of HBP at the film surface, resulting in an increased fluorophore composition.

3.3   Fluorescence Sensing

The sensing properties of the electrospun membranes were also probed. The first issue was the determination of HBP stability in the membranes. Because the HBPs do not form entanglements like linear polymers, there was potential for the loss of HBP as the membrane was subjected to different solutions and cleaning washes. Figure 6 compares the performance of the HBP-PBA
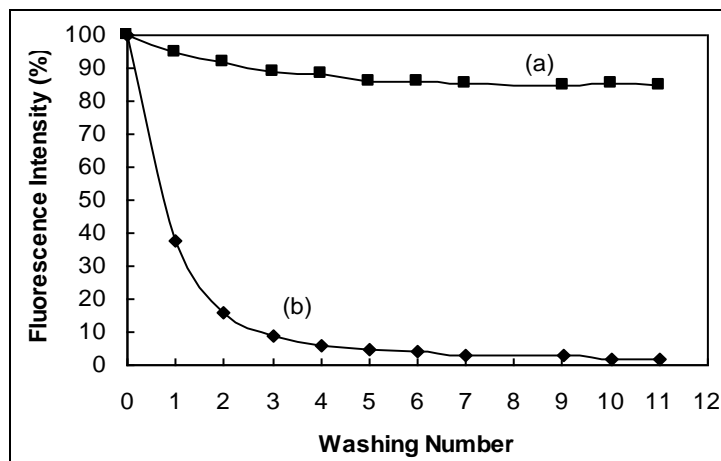
Figure 6. HBP-PBA stability in the membrane.

loaded in PHEMA and the small molecule PBA loaded in the same matrix. The electrospun membranes were washed with deionized water several times, and the loss of the HBP-PBA was much less than the small molecule fluorophore. The level of the HBP-PBA stabilized after several washings (a), indicating any loosely bound HBP-PBA had been removed under these conditions. The small molecule pyrene (b) was fully removed from the linear polymer after a few washings. The net HBP-PBA loss was ~15% of the initial loading. This evidence indicates that even without long chain entanglements, the HBP is sufficiently secure in the polymer matrix and that minimal loss is expected over short time frames.

The use of the electrospun membranes as sensors was investigated using the electron-deficient metal cation Hg(II) and the electron transfer protein cytochrome *c* (cyt *c*). Cyt *c* is a heme-containing respiratory protein, and its detection has become standard practice to confirm a myocardial infarction and to monitor patient response to treatment. In our work, the quenching behaviors of the sensors were studied by the measurement of the fluorescence spectra (intensity) of the sensing films as a function of quencher concentrations. Figure 7 shows the fluorescence spectra of three membranes varying with the concentration of cyt *c*. The results showed that the fluorescence intensity decreased with increasing concentration of cyt *c*. Similar behaviors were observed for Hg(II). Here the quenching of fluorescence is due to the interactions of an electron-rich PBA indicator[(-)] and electron deficient quencher[(+)], and the degree of quenching depends on the amount of analyte. The diffusion-controlled quenching process can be described by the Stern-Volmer bimolecular quenching kinetics (*32*).

$$F + hv \rightarrow F^*. \tag{1}$$

$$F^* \rightarrow F + hv'. \tag{2}$$

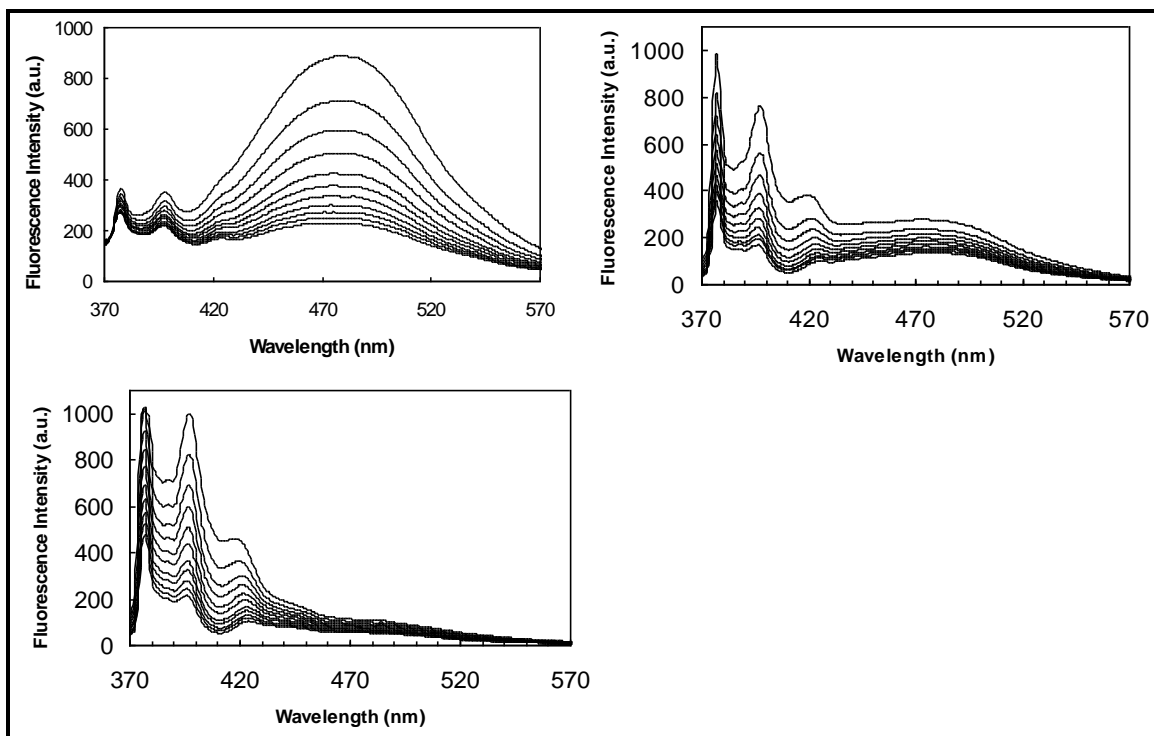$$F^* + Q \rightarrow F + Q. \tag{3}$$

11

Figure 7. HBP-PBA fluorescence quenching upon addition of *cytochrome c*. Top left, polymer 1; top right, polymer 2; bottom, polymer 3.

The fluorescent molecule F absorbs a photon to give F*, or the excited state of the fluorophore. From the excited state, F* can return to the ground state by two mechanisms. The first route emits a photon, *hv'*, to return F* to the ground state. Alternately, F* can interact with a quencher molecule Q, transferring the excitation energy and returning to the ground state without the emission of fluorescence. The quantitative measure of fluorescence quenching is described by the Stern-Volmer constant, K_{sv}, in equation 4:

$$I_0/ I = 1 + K_{sv} [Q] . \tag{4}$$

In equation 4, I_0 and I are the intensities of fluorescence in the absence and in the presence of the quencher, respectively. The equation reveals that I_0/I increases in direct proportion to the concentration of the quencher. When all other variables are held constant, the higher the K_{sv}, the lower the concentration of quencher required to inhibit fluorescence. The constant K_{sv} defines the efficiency of quenching and is given by equation 5:

$$K_{sv} = k_2\tau_1 . \tag{5}$$

In the equation, τ_1 is the luminescence decay time of the fluorophore in the absence of the quencher ($=1/k_1$), and k_2 is the bimolecular quenching rate constant. The terms defining K_{sv} imply two important practical consequences. First, the sensitivity of the quenching process is

enhanced by fluorophores with long luminescence decay times (τ_1). Second, the sensitivity of the process can be tailored by controlling the quencher diffusion rate to fluorophores via the microstructural properties of the sensing film. Fluorescence quenching is also a widely used method to study the accessibility of fluorophores to quenchers (*33*). Useful information about the microenvironment and the physical state of the fluorophore may be obtained from these kinds of studies. A linear Stern-Volmer plot indicates that the fluorophores are uniformly accessible to quencher. Nonlinear plots may arise if fluorophore accessibility to the quencher is not constant (e.g., interior and exterior residues of a folded protein) or if more than one fluorophore contributes to the fluorescence intensity of the system.

The data obtained by performing a Stern-Volmer analysis in each electrospun sensor are shown in figure 8. For Hg(II) concentrations in the range of 1×10^{-4} to 7×10^{-4} mol/l, linear plots between the concentration of quencher and I_0/I are obtained showing a Stern-Volmer relationship. Stern-Volmer constants (K_{sv}) of the electrospun films, calculated from slopes of the plots, were found to be 3.3×10^3 M^{-1}, 1.8×10^3 M^{-1}, and 1.3×10^3 (M^{-1}) for sample 3-B, 2-B, and 1-B, respectively. Table 2 shows the summary of the K_{sv} values of all the samples by Hg(II). Figure 8 depicts the Stern-Volmer plots of the quenching of the fluorescence from three samples by cyt *c*. It reveals that the quenching efficiency of cyt *c* is significantly higher than that of Hg(II). Although the plots show no linearity in the concentration range from 1×10^{-6} M to 1×10^{-5} M, the regularities are maintained in the whole concentration ranges. This nonlinearity of the plot might be due to the occurrence of more than one photo-quenching process. These results also suggest that the accessibility of the fluorophore to a large quencher like cyt *c* would be lower than that to a small quencher like Hg(II) due to increased steric interactions. A lower concentration of fluorophore is advantageous for the sensitivity of the sensor. There is no significant difference when using different polymer matrices—in this case, PHEMA and PAN.
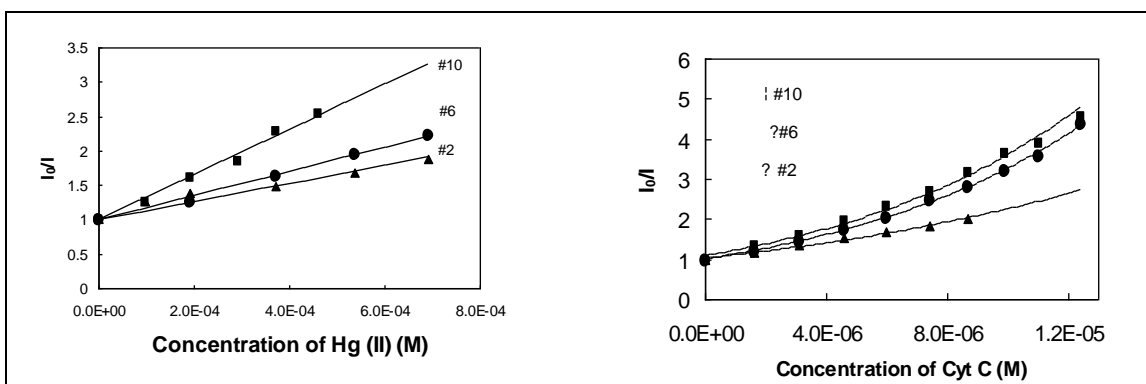

Figure 8. HBP-PBA sensitivity by analyte.

Table 2. Performance of electrospun membrane sensors.

Sample	HBP	Matrix	Mass% HBP	Mass% PBA	K_{sv} Hg(II)[*]
1-A	1	PHEMA	1	0.144	1.5
1-B	1	PHEMA	4	0.576	1.3
1-C	1	PAN	1	0.144	1.4
1-D	1	PAN	4	0.576	1.3
2-A	2	PHEMA	1	0.0772	2.2
2-B	2	PHEMA	4	0.309	1.8
2-C	2	PAN	1	0.0772	2.0
2-D	2	PAN	4	0.309	1.9
3-A	3	PHEMA	1	0.0199	3.5
3-B	3	PHEMA	4	0.0796	3.3
3-C	3	PAN	1	0.0199	3.4
3-D	3	PAN	4	0.0796	3.1

[*]Summary of electrospun membrane sensitivity towards Hg^{2+} cations.

4. Conclusions

The development of fluorescence quenching–based sensors using HBP-based fluorophores was demonstrated in this report. Low concentrations of fluorophore were transported to the surface of electrospun membranes by thermodynamic driving forces, and a high accessibility of the fluorophores to quenching agents was demonstrated. The Stern-Volmer constant for the quenching of the fluorophores ranged from 1.3 to 3.5×10^3. While these values are modest, we found that lower concentrations of fluorophore on the periphery of the HBP responded more strongly to the analytes. Both Hg(II) and cytochrome *c* were used to test the sensing capability of the fluorophore, and fluorescence intensity was found to respond to concentration changes for both the small quencher (Hg) and the large molecule quencher (cyt *c*).

5.   References

1.   Yang, J. S.; Swager, T. M. Fluorescent Porous Polymer Films as TNT Chemosensors: Electronic and Structural Effects. *J. Am. Chem. Soc.* **1998**, *120*, 11864–11873.

2.   Chen, L. H.; Mcbranch, D. W.; Wang, H. L.; Helgeson, R.; Wudl, F.; Whitten, D. G. Highly Sensitive Biological and Chemical Sensors Based on Reversible Fluorescence Quenching in a Conjugated Polymer. *Proc. Natl. Acad. Sci.* **1999**, *96*, 12287–12292.

3.   Fan, C.; Plaxco, K. W.; Heeger, A. J. High-Efficiency Fluorescence Quenching of Conjugated Polymers by Proteins. *J. Am. Chem. Soc.* **2002**, *124*, 5642–5643.

4.   Wang, X. Y.; Lee, S. H.; Drew, C.; Senecal, K. J.; Kumar, J.; Samuelson, L. A. Electrospun Nanofibrous Membranes for Highly Sensitive Optical Sensors. *Nano Lett.*, **2002**, *2*, 1273–1275.

5.   Wang, X. Y.; Drew, C.; Lee, S. H.; Senecal, K. J.; Kumar, J.; Samuelson, L. A. Electrospinning Technology: A Novel Approach to Sensor Applications. *J. Macro. Sci. Pure Appl. Chem.* **2002**, *A39*, 1251–1258.

6.   Reneker, D. H.; Chun, I. Nanodiametre Diameter Fibers of Polymer, Produced by Electrospinning. *Nanotechnology* **1996**, *7*, 215.

7.   Wang, X. Y.; Kim, Y. G.; Drew, C.; Ku, B-C; Kumar, J.; Samuelson, L. A. Electrostatic Assembly of Conjugated Polymer Thin Layers on Electrospun Nanofibrous Membranes for Biosensors. *Nano Lett*. **2004**, *4*, 331–334.

8.   Wang, X. Y.; Yang, S. Z.; Drew, C.; Samuelson, L. A.; Kumar, *J. Polym. Preprints* (American Chemical Society, Division of Polymer Chemistry) **2003**, *44* (2), U442–U442.

9.   Hester, J. F.; Mayes, A. M. Design and Performance of Foul-Resistant Poly(Vinylidene Fluoride) Membranes Prepared in a Single-Step by Surface Segregation. *J. Membr. Sci.* **2002**, *202*, 119–135.

10. Schaub, T. F.; Kellogg, G. J.; Mayes, A. M.; Kulasekere, R.; Ankner, J. F.; Kaiser, H. Surface Modification via Chain End Segregation in Polymer Blends. *Macromolecules* **1996**, *29*, 3982–3990.

11. Mason, R.; Jalbert, C. A.; O'Rourke Muisener, P. A. V.; Koberstein, J. T.; Elman, J. F.; Long, T. E.; Gunesin, B. Z. Surface Energy and Surface Composition of End-Fluorinated Polystyrene. *Adv. Colloid Interface Sci.* **2001**, *94*, 1–19.

12. Wang, J.; Kara, S.; Long, T. E.; Ward, C. Synthesis of Central Functionalized Asymmetric Triblock Copolymers for Surface Modification and Switchable Surface Properties. *J. Polym. Sci., Part A: Polym. Chem.*, **2000**, *38*, 3742–3750.

13. Kim, Y. H.; Webster, O. W. Hyperbranched Polyphenylenes. *Macromolecules* **1992**, *25*, 5561–5572.

14. Malmström, E.; Johansson, M.; Hult, A. The Effect of Terminal Alkyl Chains on Hyperbranched Polyesters Based on 2,2-bis(hydroxymethyl)propionic Acid. *Macromol. Chem. Phys.* **1996**, *197*, 3199–3207.

15. Mueller, A.; Kowalewski, T.; Wooley, K. L. Synthesis, Characterization, and Derivitization of Hyperbranched Polyfluorinated Polymers. *Macromolecules* **1998**, *31*, 776–778.

16. Gan, D.; Mueller, A.; Wooley, K. L. Amphiphilic and Hydrophobic Surface Patterns Generated From Hyperbranched Fluoropolymer/Linear Polymer Networks: Minimally Adhesive Coatings via the Crosslinking of Hyperbranched Fluoropolymers. *J. Polym. Sci. Part A Polym. Chem.* **2003**, *41*, 3531–3540.

17. Beterlein, D.; Belge, G.; Eichhorn, K-J.; Gauglizt, G.; Grundke, K.; Voit, B. Preparation and Properties of Thin Films of Hyperbranched Polyesters With Different End Groups. *Macromol. Symp*. **2001**, *164*, 117–131.

18. Orlicki, J. A.; Viernes, N. O. L.; Moore, J. S.; Sendijarevic, I.; McHugh, A. J. Roles of Molecular Architecture and End-Group Functionality on the Surface Properties of Branched Polymers. *Langmuir* **2002**, *18*, 9990–9995.

19. Lange, J.; Stenroos, E.; Johansson, M.; Malström, E. Barrier Coatings for Flexible Packaging Based on Hyperbranched Resins. *Polymer* **2001**, *42*, 7403–7410.

20. Schmaljohann, D.; Pötschke, P.; Hässler, R.; Voit, B. I.; Froehling, P. E.; Mostert, B.; Loontjens, J. A. Blends of Amphiphilic, Hyperbranched Polyesters and Different Polyolefins. *Macromolecules* **1999**, *32*, 6333–6339.

21. Hong, Y.; Cooper-White, J. J.; Mackay, M. E.; Hawker, C. J.; Malmström, E.; Rehnberg, N. A Novel Processing Aid for Polymer Extrusion: Rheology and Processing of Polyethylene and Hyperbranched Polymer Blends. *J. Rheol.* **1999**, *43*, 781–793.

22. Hong, Y.; Coombs, S. J.; Cooper-White, J. J.; Mackay, M. E.; Hawker, C. J.; Malmström, E.; Rehnberg, N. Film Blowing of Linear Low-Density Polyethylene Blended With a Novel Hyperbranched Polymer Processing Aid. *Polymer* **2000**, *41*, 7705–7713.

23. Orlicki, J. A.; Moore, J. S.; Sendijarevic, I.; McHugh, A. J. Role of End-Group Functionality on the Surface Segregation Properties of HBPs in Blends With Polystyrene: Application of Hbps as Dewetting Inhibitors. *Langmuir* **2002**, *18*, 9985–9989.

24. McNamara, J. J.; Gupta, A.; Devore, D. Hyperbranched Amphiphilic Polymeric Additives and Polymer Compositions With Increased Surface Energy. U.S. Patent 6,444,758, September 3, 2002.

25. Orlicki, J. A.; Kosik, W. E.; Demaree, J. D.; Bratcher, M. S.; Jensen, R. E.; McKnight, S. H. Surface Segregation of Branched Polyethyleneimines in a Thermoplastic Polyurethane. *Polymer* **2007**, *48*, 2818–2826.

26. Hunley, M. T.; Harber, A.; Orlicki, J. A.; Rawlett, A. M.; Long, T. E. Effect of Hyperbranched Surface-Migrating Additives on the Electrospinning Behavior of Poly(Methyl Methacrylate). *Langmuir* **2008**, *24*, 654–657.

27. Pugh, V. J.; Hu, Q. S.; Pu, L. The First Dendrimer-Based Enantioselective Fluorescent Sensor for the Recognition of Chiral Amino Acids. *Angew. Chem., Int. Ed. Engl.* **2000**, *39*, 3638–3641.

28. Pugh, V. J.; Hu, Q. S.; Zuo, X. B.; Lewis, F. D.; Pu, L. Optically Active BINOL Core-Based Phenyleneethynylene Dendrimers for the Enantioselective Fluorescent Recognition of Amino Alcohols. *J. Org. Chem.* **2001**, *66*, 6136–6140.

29. Johansson, M.; Malmström, E.; Hult, A. Synthesis, Characterization, and Curing of Hyperbranched Allyl Ether Maleate Functional Ester Resins. *J. Polym. Sci. Part A, Polym. Chem.* **1993**, *31*, 619–624.

30. Jannasch, P. Surface Structure and Dynamics of Block and Graft Copolymers Having Fluorinated Poly(Theylene Oxide) Chain Ends. *Macromolecules* **1998**, *31*, 1341–1347.

31. Bottino, F. A.; Di Pasquale, G.; Pollicino, A.; Pilati, F.; Toselli, M.; Tonelli, C. XPS Study on Surface Segregation in poly(ethylene-isoterephthalate)-perfluoropolyether Block Copolymers. *Macromolecules* **1998**, *31* (22), 7814–7819.

32. Turro, N. J. *Modern Molecular Photochemistry*; The Benjamin/Cummings Publishing Co.: Menlo Park, CA, 1978.

33. Lakowicz, J. R. *Principles of Fluorescence Spectroscopy*; Academic/Plenum Publishers: New York, 1999.